Three conformational states of scallop myosin S1

A. Houdusse*†‡, A. G. Szent-Györgyi§, and C. Cohen*†

*Rosenstiel Basic Medical Sciences Research Center, and §Biology Department, Brandeis University, Waltham, MA 02254-9110

Contributed by Carolyn Cohen, August 9, 2000

We have determined the structure of the intact scallop myosin head, containing both the motor domain and the lever arm, in the nucleotide-free state and in the presence of MgADP·VO4, corresponding to the transition state. These two new structures, together with the previously determined structure of scallop S1 complexed with MgADP (which we interpret as a detached ATP state), reveal three conformations of an intact S1 obtained from a single isoform. These studies, together with new crystallization results, show how the conformation of the motor depends on the nucleotide content of the active site. The resolution of the two new structures (≈4 Å) is sufficient to establish the relative positions of the subdomains and the overall conformation of the joints within the motor domain as well as the position of the lever arm. Comparison of available crystal structures from different myosin isoforms and truncated constructs in either the nucleotide-free or transition states indicates that the major features within the motor domain are relatively invariant in both these states. In contrast, the position of the lever arm varies significantly between different isoforms. These results indicate that the heavy-chain helix is pliant at the junction between the converter and the lever arm and that factors other than the precise position of the converter can influence the position of the lever arm. It is possible that this pliant junction in the myosin head contributes to the compliance known to be present in the crossbridge.

Recent results on the myosin motor are beginning to reveal how this machine transforms chemical energy into movement. Crystallographic and biochemical studies on a number of isoforms (1–6) have identified at least three conformational states of the motor, which appear to correspond to different steps in the actomyosin cycle. The first crystal structure determined was that of methylated chicken skeletal muscle S1 without nucleotide (which contains a SO_4^{2-} ion in the active site; ref. 1). Although not bound to actin, this structure was considered to correspond closely to the postpower stroke (or rigor state), because the lever arm is in the "down" position (at an angle of ≈45° to the actin filament axis). This remarkable structure also led to the concept that the movement of the light-chain-bearing lever arm is responsible for force production and motility. Next, the structures of an expressed *Dictyostelium* motor domain (MD; lacking the lever arm) complexed with various nucleotide analogs were determined—often at high resolution (2–4). This work revealed detailed images of the nucleotide-binding site and led to the concept of myosin as a "back door" enzyme. The truncated structures fell into two classes, which were interpreted differently by Gulick and Rayment (7) and by Holmes (8). The latter author modeled one class of structures as corresponding to the "primed" or transition state, where the lever arm (if present) would be in an "up" position (at ≈90° to the actin filament axis), and the other class would be in the down position similar to that of the postpower stroke state. However, the fact that ATP analogs (2) also yielded this state led Gulick and Rayment (7) to consider that this down position of the lever arm (also found in the methylated nucleotide-free chicken skeletal S1 structure) could correspond to a weak—rather than a strong—actin-binding state that differed in structure from the postpower stroke state. Thus, a number of conflicting findings—often from different isoforms or truncated constructs—have prevented a simple interpretation of some of these results. More recent studies with an expressed vertebrate smooth muscle MD-essential light-chain complex (MDE) have revealed the lever-arm position in the primed or transition state for the first time (5), which corresponds well with the modeling study of Holmes (8). During the past year, a third conformational state has been discovered by the structure determination of an intact, unmodified scallop S1 complexed with MgADP (6). This study determined that the lever arm is in an unusual orientation compared with the down position and is quite near the actin filament and almost parallel to its axis. Moreover, the SH1 helix is unwound. This latter feature had not been seen in any previous structure. This newly discovered structure has been interpreted as corresponding to a detached stable ATP state that occurs between the rigor and transition states.

Here, we describe, at low resolution (≈4 Å), two structural states previously not seen in intact scallop S1. These results, together with the unusual conformation we have recently reported (6), demonstrate how the intact head of a single myosin isoform undergoes critical conformational changes that correspond to three distinct steps in the contractile cycle. One of the states we describe corresponds to a nucleotide-free structure with the lever arm in the postpower stroke (≈45°) orientation. New crystallization results do not support earlier interpretations (7) that this structure might correspond to a stable ATP state. We find that, for each structural state, the position of the subdomains and the conformation of the joints within the MD (see Fig. 1 and ref. 6) are relatively invariant between the available crystal structures of different myosin isoforms. In contrast, the position of the lever arm varies significantly when structures of different myosin isoforms are compared in both the nucleotide-free and transition states. This finding shows that the position of the lever arm can be modulated by various interactions with little change in the MD conformation. This study supports the conclusion that the distinct structural states observed in an intact, unmodified myosin head depend on the specific nucleotide or nucleotide analog that is bound. Moreover, we have identified a short pliant junction at the beginning of the lever-arm helix that may play a critical role in the mechanical properties of the myosin head.

Methods

Crystallization and Data Collection. S1 from scallop (*Argopecten irradians*) striated muscle myosin was obtained as described (6). Crystals of nucleotide-free S1 (near-rigor state) grew in a day at 4°C in hanging drops containing equal amounts of reservoir

Abbreviations: MD, motor domain; MDE, MD-essential light-chain complex; ELC, essential light chain.

Data deposition: The atomic coordinates have been deposited in the Protein Data Bank, www.rcsb.org (PDB ID codes 1dfl for nucleotide-free scallop S1 and 1dfk for scallop S1-VO4).

†To whom reprint requests should be addressed. E-mail: ccohen@brandeis.edu or Anne.Houdusse@curie.fr.

‡Present Address: Structural Motility Institut Curie, Centre National de la Recherche Scientifique, Unité Mixte de Recherche 144, 26 Rue d'Ulm, 75248 Paris cedex 05, France.

The publication costs of this article were defrayed in part by page charge payment. This article must therefore be hereby marked "*advertisement*" in accordance with 18 U.S.C. §1734 solely to indicate this fact.

Article published online before print: *Proc. Natl. Acad. Sci. USA*, 10.1073/pnas.200376897. Article and publication date are at www.pnas.org/cgi/doi/10.1073/pnas.200376897

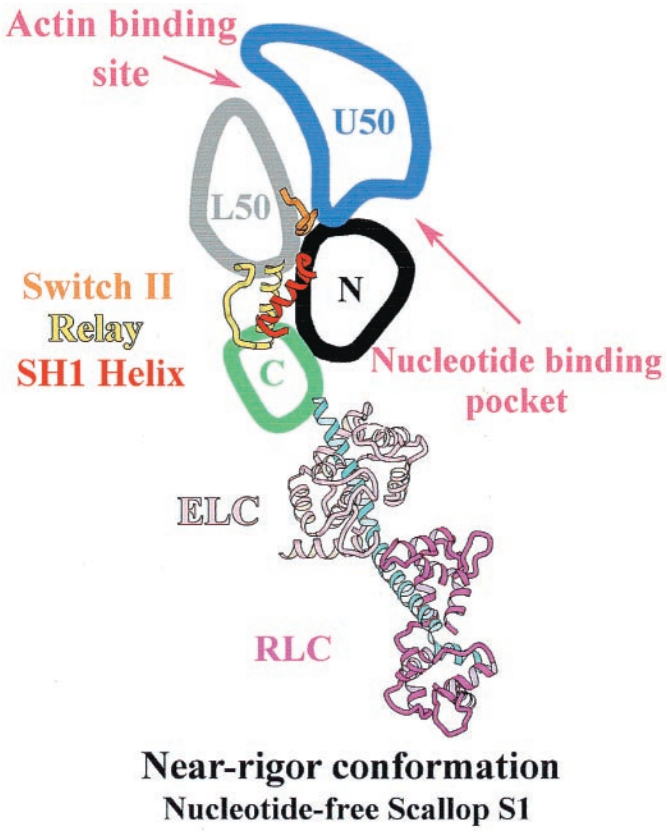

Fig. 1. Schematic drawing of the subdomains within the myosin head in the nucleotide-free scallop S1 structure. The four subdomains of the MD are labeled, as are three structural elements (joints) that articulate movements within the head: switch II (residues Ile-461 to Asn-470, orange); the relay (residues Asn-489 to Asp-515, yellow); and the SH1 helix (Cys-693 to Phe-707, red). Note that in all figures, the same colors have been kept for the four subdomains of the MD: the N-terminal (black), upper 50-kDa subdomain (blue), lower 50-kDa subdomain (gray), and the converter (green) as well as for the three joints. ELC, essential light chain; RLC, regulatory light chain.

solution [50 mM cacodylate, pH 7.0/50 mM $(NH_4)_2SO_4$/10 mM $MgCl_2$/15% (vol/vol) glycerol/≈7% (vol/vol) polyethylene glycol 8000] and protein solution (20 mg/ml). These crystals belong to space group $P2_1$ (a = 86.5 Å, b = 52.1 Å, c = 164.6 Å, β = 100.3°) with one molecule per asymmetric unit. Crystals of S1 complexed with MgADP·VO_4 (transition state) were obtained at 4°C by microseeding sitting drops containing equal amounts of reservoir solution [7% (vol/vol) polyethylene glycol 8000/50 mM Mes, pH 6.0/3 mM $MgCl_2$] and protein solution (20 mg/ml of S1 and 0.5 mM MgADP·VO_4). The crystals belong to space group $P2_1$ (a = 53.3 Å, b = 243.5 Å, c = 124.6 Å, β = 100.2°) with two molecules per asymmetric unit. Crystals of the third or detached state, as discussed in ref. 6, grew under different conditions, by microseeding sitting drops containing equal amounts of reservoir solution [6% (vol/vol) polyethylene glycol 20,000/100 mM Tris, pH 8.0/12% (vol/vol) glycerol] and protein solution (20 mg/ml S1 complexed with 4 mM MgADP, 4 mM MgADP·BeF_x, or 4 mM MgAMPPNP (adenylyl-imidodiphosphate).

By using glycerol as a cryoprotectant, a data set was collected at 100 K (Cornell High Energy Synchrotron Source beamline A1; λ = 0.90 Å) to 4.2-Å resolution for a nucleotide-free crystal and to 3.8-Å resolution for two S1-VO_4 crystals. The data sets were indexed and scaled with DENZO and SCALEPACK (9). For the nucleotide-free S1 crystal, scaling of 139,608 observations resulted in a 97.9% complete data set of 10,676 reflections with an R_{merge} of 6.3%. For the transition-state crystals, scaling of 426,824 observations resulted in a 95.5% complete data set of 29,173 reflections with an R_{merge} of 9.8%. The averaged I/σ ratio is 27 in the case of the nucleotide-free crystal for reflections between 30 and 4.2 Å and 20.4 in the case of the transition-state crystals for reflections between 40 and 3.8 Å.

Structure Determination and Refinement. The molecular replacement solution was found with the program AMoRe (10). The search models used were two separate components of the crystallographic model of scallop S1-ADP (PDB-code 1B7T): the lever arm and the MD; in the latter component, 25 residues of the relay and 83 residues of the SH1 helix region and the converter were excluded. Side chains were removed from the models because of the limited resolution of the data. The FITING routine of AMoRe was used for rigid body refinement of the model, which was divided into 12 parts for the nucleotide-free structure and 16 for the transition-state structure. After convergence, the subdomains of the MD adopt positions similar to those observed in other structures (such as chicken skeletal S1 for the nucleotide-free scallop S1 and smooth muscle MDE-AlF_4^- for scallop S1-VO_4). The electron density map calculated by using phases from these models revealed clear density that allowed us to position both the converter and the relay and indicated that the SH1 helix was intact in both structures. Model building was performed with the program O (11). Near the nucleotide-binding site, the density was of poor quality in the case of the nucleotide-free structure, and 26 residues were removed, including switch I. In contrast, the density was of good quality for this region in the case of the S1-VO_4 structure, including that of the MgADP·VO_4 ligand. The final model for the nucleotide-free structure has an R_{factor} of 41.5% at 4.2-Å resolution; that of scallop S1-VO_4 has an R_{factor} of 39.4% at 3.8-Å resolution. (Note that positional refinement cannot be carried out because of the limited resolution of the data.) The quality of the electron density map, which allowed us to visualize the position of the relay, the SH1 helix, and the converter, validates these low-resolution models. Note also that starting from various atomic models, in the detached, transition-state, or near-rigor conformations, the rigid body refinement always converged for new positions of the so-called "N-terminal," "upper," and "lower" 50-kDa subdomains of the MD (see Fig. 1) that correspond to a near-rigor conformation in the case of data from the nucleotide-free crystal and a transition-state conformation in the case of S1-VO_4 crystals. Thus, the rms deviation for about 500 Cα positions of equivalent residues of these three subdomains is only 0.97 Å between nucleotide-free chicken and scallop S1 and 1.0 Å between smooth MDE-AlF_4^- and scallop S1-VO_4. The rms deviation for these same atomic positions between scallop S1-ADP (used as the first model to solve the structure by molecular replacement) and nucleotide-free S1 is 1.72 Å and is equal to 2.64 Å when scallop S1-VO_4 and scallop S1-ADP (detached state) are compared.

Other Crystallization Experiments. Using each of the three crystallization conditions discussed above (producing the near-rigor, detached, and transition-state structures), we examined a number of other nucleotides or their analogs to determine which crystals they produced (if any). By using the near-rigor conditions, crystals similar to the near-rigor state could be obtained with MgADP. However, S1 complexed with either ATP analogs (MgAMPPNP, MgADP·BeF_x) or ADP·Pi analogs (MgADP·VO_4, MgADP·AlF_4^-) did not produce crystals. In contrast, by using the appropriate crystallization conditions, transition-state crystals were obtained for S1 complexed with MgADP·AlF_4^-. However, no crystals grew without nucleotide present or when S1 was complexed with MgADP or ATP analogs. By using detached-state conditions, crystals of S1 complexed with ATP analogs were obtained, but no crystals

were obtained with scallop S1 when no nucleotide was bound or when the S1 was complexed with transition-state analogs.

Results and Discussion

Correspondence Between the Conformation of the Myosin Head and the Nucleotide Content of Its Active Site. We have shown that scallop S1 crystallizes in three different crystal forms depending on the content of the nucleotide-binding pocket. Different ionic and pH conditions (see *Methods*) are required for the growth of each of these crystal forms, probably reflecting differences in interactions between neighboring molecules. We have solved these stuctures, which correspond to three distinct conformational states of the motor. In this respect, scallop is a privileged system, because it allows one to test which conformation exists with a particular nucleotide bound to S1. The first structure (called near-rigor by us) was that of nucleotide-free scallop S1, determined to 4.2-Å resolution. This structure could also be obtained in the presence of MgADP, as reported for *Dictyostelium* myosin II (4). The second structure is that of S1 complexed with MgADP·VO4 (S1-VO_4), determined to a resolution of 3.8 Å, and corresponds to a transition-state structure, required for hydrolysis of ATP (2). Crystals of this form could be obtained only when scallop S1 was complexed with ADP·Pi analogs. The third structure, obtained under different conditions (see *Methods* and ref. 6), is that of S1 complexed with MgADP (S1-ADP), determined to 2.5-Å resolution (6), which we believe corresponds to a new detached ATP state of the actomyosin cycle. Crystals with unit cell parameters similar to this form also grew when S1 was complexed with ATP analogs but not in the absence of nucleotide or when S1 was complexed with ADP·Pi analogs. Using scallop S1, we have thus shown the link between a particular nucleotide (or its absence) in the active site and the conformational state of an intact unmodified myosin head (i.e., with a complete lever arm) from a single isoform. We must emphasize, however, that these crystallographic results, obtained in the absence of actin, including the case of the near-rigor nucleotide-free S1, do not define the conformation of the strong binding states of S1.

A Simple Description of the MD Arrangement. As proposed in Houdusse *et al.* (6), the motor of the S1 structure is most simply described as being made up of four major subdomains (see Fig. 1) that are linked by three single-stranded joints. In the transition between states, coordinated changes in the conformation of the joints are associated with rigid body movements of the four subdomains. The region of the motor that shows the greatest positional change in the three conformations is one of these subdomains, which is called the "converter" (12), that immediately adjoins the lever arm. The other subdomains show only small changes in position in different states. The movements of the converter are directly coupled to and amplified by the extended lever arm. One of the joints, the "relay", has strong connections to the converter and controls its movement. Different orientations of the converter/relay module (produced by conformational changes at both ends of the relay) characterize the different structural states. A 15-residue-long region before the converter constitutes a second joint—the so-called "SH1 helix region"—whose conformation depends on the different orientations of the converter. Nucleotide binding promotes the unwinding of the helix, uncoupling the converter from the rest of the MD. Switch II is a third joint, near the γ-phosphate pocket and positioned at the bottom of the actin-binding cleft. This joint plays a critical role in the communication between the nucleotide-binding site and the actin-binding interface. In the transition between states, the three joints act together to control the overall organization of the myosin head. This arrangement allows direct communication between distant critical regions of the head, such as the nucleotide-binding site, the actin-binding interface, and the lever arm.

The Scallop MD in the Three States. Despite the low resolution of the two new structures of scallop S1 (Fig. 2*A*), which precludes identification of side-chain interactions, the quality of the electron density allows us to establish the relative positions of the subdomains within the MD as well as the overall conformation of the joints within the motor (Fig. 2 *B* and *C*). These features allow us to assign conformational states without ambiguity. The nucleotide-free structure corresponds to a near-rigor conformation previously observed at higher resolution in the methylated nucleotide-free chicken skeletal S1 structure (1) and in the truncated MD of *Dictyostelium* myosin II complexed with ATP analogs (2, 4). Note, however, that in contrast to the results of Rayment and colleagues (refs. 2 and 4; see also ref. 7), scallop S1 complexed with ATP analogs did not crystallize in near-rigor conditions (see *Methods*), suggesting that this near-rigor conformation is not compatible with a stable ATP state. The scallop S1-VO_4 structure corresponds to a transition-state conformation previously described at higher resolution in the structures of *Dictyostelium* myosin II MD complexed with ADP·Pi analogs (2, 3) and smooth muscle MD and MDE bound to MgADP·AlF_4^- (5).

There are striking differences that distinguish the three structural states. In particular, the three states differ greatly in the position of the converter (and thus the light-chain binding domain or lever arm) as well as in the conformation of the actin-binding interface. The converter rotates about 65° between the transition and nucleotide-free states of scallop S1 and leads to a movement of the lever arm between these states that has a very small azimuthal component (see Fig. 2*C*). In both these structures, the SH1 helix is intact, and the four subdomains are closely linked. By contrast, the detached ATP conformation (seen in scallop S1-ADP) is characterized by subdomains that are loosely coupled, because the SH1 helix is unwound (6). Correspondingly, the position of the converter/relay module is not constrained and various orientations of this module compared with the other subdomains of the MD could lead to a number of possible positions of the lever arm relative to the MD. In the scallop S1-ADP crystal structure, for example, the converter has rotated by about 30° from the position seen in the near-rigor structure, and the lever arm is almost parallel to the actin filament axis (Fig. 3). The changes in switch II—which affect only five residues—are surprisingly small considering that their structural effects are very large. Thus, in both the near-rigor and detached conformations, in which the 50-kDa cleft is open, this joint seems to be very similar. In the transition-state conformation, however, switch II has moved toward the nucleotide-binding site, and thus closes the bottom of the 50-kDa cleft, preventing phosphate release (2). These relatively invariant features of the MD in myosins from different isoforms allow one to classify structures in different conformational states.

A Pliant Region at the Junction Between the MD and Lever Arm. In contrast to the strong conservation of the features in the MD, the exact position of the lever arm can vary greatly among structures in the same state but from different isoforms and from different constructs. In the near-rigor conformation, the orientation of the lever arm of scallop and chicken skeletal S1 differ by 40°, taking into account both the azimuthal and axial components (see Fig. 2 *B* and *C*). Because of the axial component (about 25°), the scallop lever arm is positioned closer to the actin filament than that of chicken skeletal S1 (see Fig. 2*B*). The difference in the lever-arm position is even more striking when one compares scallop S1 and chicken smooth MDE in the transition-state conformation. The orientations of their lever arm differ by about 65°, with a major component perpendicular to the actin filament axis (see Fig. 2 *B* and *C*). These differences arise because of two

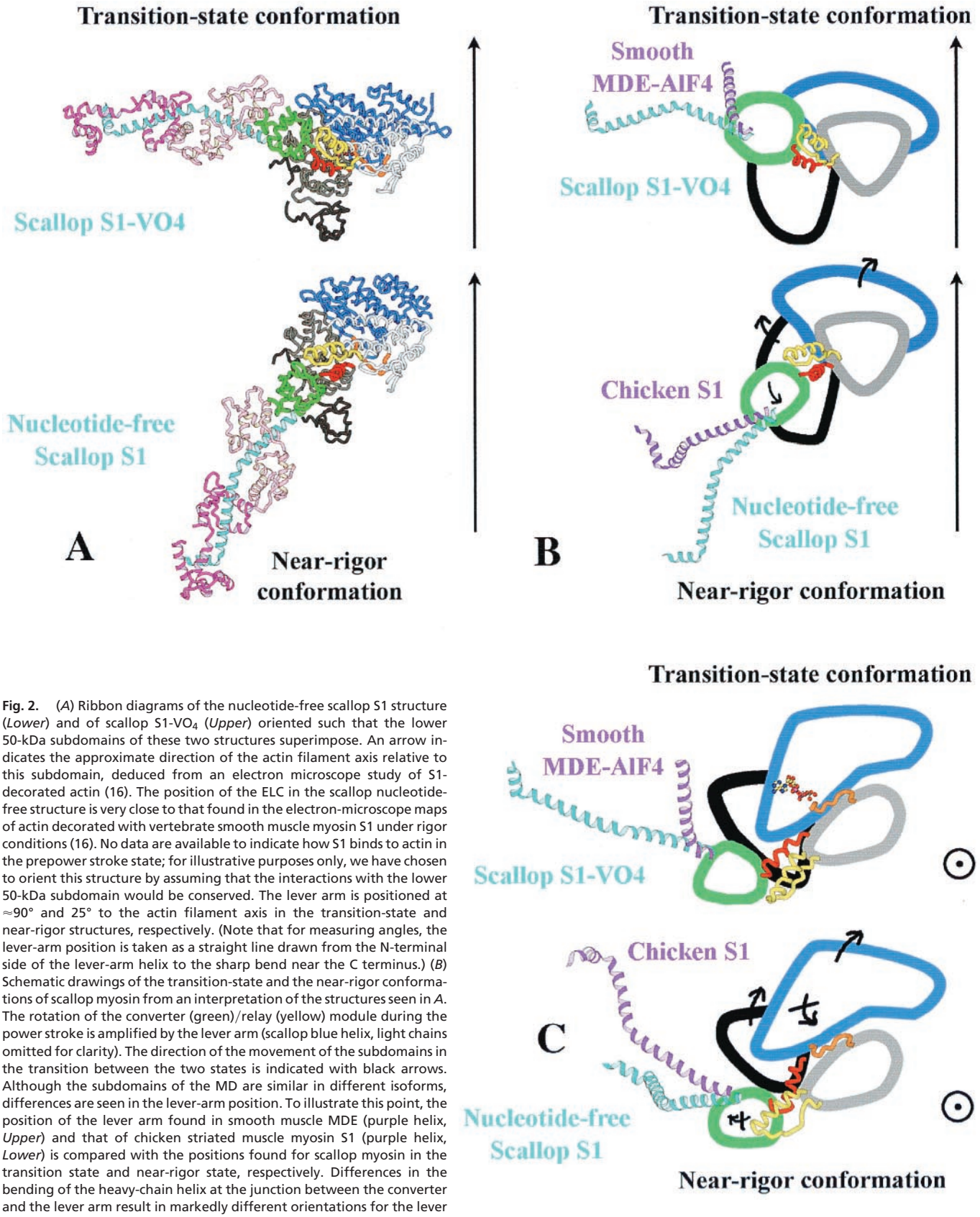

Fig. 2. (*A*) Ribbon diagrams of the nucleotide-free scallop S1 structure (*Lower*) and of scallop S1-VO_4 (*Upper*) oriented such that the lower 50-kDa subdomains of these two structures superimpose. An arrow indicates the approximate direction of the actin filament axis relative to this subdomain, deduced from an electron microscope study of S1-decorated actin (16). The position of the ELC in the scallop nucleotide-free structure is very close to that found in the electron-microscope maps of actin decorated with vertebrate smooth muscle myosin S1 under rigor conditions (16). No data are available to indicate how S1 binds to actin in the prepower stroke state; for illustrative purposes only, we have chosen to orient this structure by assuming that the interactions with the lower 50-kDa subdomain would be conserved. The lever arm is positioned at ≈90° and 25° to the actin filament axis in the transition-state and near-rigor structures, respectively. (Note that for measuring angles, the lever-arm position is taken as a straight line drawn from the N-terminal side of the lever-arm helix to the sharp bend near the C terminus.) (*B*) Schematic drawings of the transition-state and the near-rigor conformations of scallop myosin from an interpretation of the structures seen in *A*. The rotation of the converter (green)/relay (yellow) module during the power stroke is amplified by the lever arm (scallop blue helix, light chains omitted for clarity). The direction of the movement of the subdomains in the transition between the two states is indicated with black arrows. Although the subdomains of the MD are similar in different isoforms, differences are seen in the lever-arm position. To illustrate this point, the position of the lever arm found in smooth muscle MDE (purple helix, *Upper*) and that of chicken striated muscle myosin S1 (purple helix, *Lower*) is compared with the positions found for scallop myosin in the transition state and near-rigor state, respectively. Differences in the bending of the heavy-chain helix at the junction between the converter and the lever arm result in markedly different orientations for the lever arm of these structures representing the same state. (*C*) Schematic drawing of an orthogonal view of the structures seen in *A*. In this orientation, the actin filament axis is approximately perpendicular to the page, and one can thus estimate the azimuthal component of the movement of the lever arm. This component is very small in the case of scallop. In contrast, bending of the heavy-chain helix at the pliant region in smooth MDE in the transition-state conformation could lead to a large azimuthal component during the power-stroke in this myosin. Comparison of the transition-state and near-rigor conformations in this view reveals changes in the position of the upper and lower 50-kDa subdomains related to differences in both the conformation of switch II and the actin-binding site.

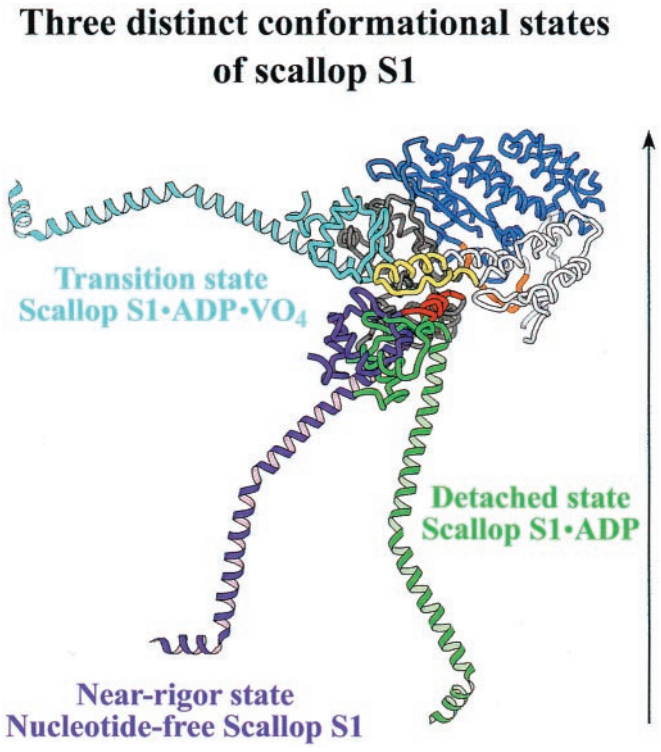

Fig. 3. Ribbon diagrams of the nucleotide-free scallop S1 structure in near-rigor, transition, and detached states, oriented such that the lower 50-kDa subdomains of these three structures superimpose. An arrow indicates the approximate direction of the actin filament axis relative to this subdomain, deduced from electron microscope studies (13, 16). The light chains bound to the heavy-chain helix of the lever arm in these three structures are omitted for clarity. Large differences are found in the position of the converter and result from relatively small rearrangements of the other three subdomains of the MD (not shown). In the three scallop S1 structures, the heavy-chain helix is straight at the junction between the converter and the lever arm, and the interactions at the interface between the converter and the ELC seem to be conserved.

structural features: a minor one is the small difference (about 12°) in the orientation of the converter/relay module, but the major one is the presence of a relatively small, unstabilized, and hence pliant region (residues Asp-775 to Lys-780, scallop sequence) in the heavy-chain helix at the junction between the converter and the lever arm in all three isoforms.

In the three conformational states of scallop S1, the heavy-chain helix is straight at this point, and the converter/ELC interactions seem to be maintained. Note that in the three scallop crystal forms, the lever arm does not interact strongly with neighboring molecules. In the head of this myosin isoform, the converter thus moves the lever arm without the pliant region flexing when other forces are not applied to the lever arm. In the other two myosin isoforms, the heavy-chain helix is not straight at the pliant region, but because these myosin heads have been observed in only one conformational state, we do not yet know what bends might occur in the other states. In fact, the large heavy-chain bend at the pliant region observed in the crystal structure of the transition state of chicken smooth MDE (5) does not seem to be present in the lower-resolution electron-microscope images of the postpower stroke states of this myosin bound to actin (16). Note, however, that in all cases, the converter/ELC interactions (which affect the degree of bending at the pliant region) are weak and differ in the states observed in these three myosin isoforms (6). The key point illustrated by these differences is that the position of the lever arm may be modulated by factors other than the precise position of the converter. The design of this region of the myosin head could thus play a key role in the elastic properties of the crossbridge (17).

The Three Conformational States and the Actomyosin Cycle. The three crystal structures described herein for scallop myosin are all observed in the absence of actin, and none can represent a strong actin-binding state of the myosin motor. The transition-state conformation, in which the lever arm is primed, corresponds to the prepower stroke state that binds actin weakly, before phosphate release. And, as described in ref. 6, we believe that the conformation of scallop S1 complexed with MgADP (in which the SH1 helix is melted) corresponds to a weakly bound, long-lived ATP state of myosin, which promotes the dissociation of myosin from actin.

The general orientation of the lever arm in the nucleotide-free structures of both chicken and scallop S1 that corresponds to the near-rigor conformation resembles that found in three-dimensional reconstructions of S1-actin complexes (13). This conformation cannot, however, correspond to a strong actin-binding state, because it does not account for actin-induced changes in S1. Kinetic studies show that binding of a nucleotide-free head to F actin is a two-step process that includes a temperature-dependent conformational change (14, 15, 21). Note that whatever structural rearrangements occur on the strong binding of actin to S1, they should greatly reduce the affinity of the myosin head for a nucleotide. With our current understanding of the dynamics in the myosin head, we expect that the actin-binding cleft and the nucleotide-binding pocket might differ between the true actin-bound rigor state and the non-actin-bound near-rigor state, but the conformation of the relay, the SH1 helix, the converter, and the lever arm would be similar. Actin is thus likely to induce subdomain movements that have not yet been described in the three known myosin states, such as movements of the upper 50-kDa subdomain relative to the N-terminal subdomain or movements within the upper 50-kDa subdomain. In our view, the near-rigor conformation might correspond to a transient state of the motor that occurs initially on ATP binding to acto-S1. Our studies on scallop myosin suggest, however, that this state is likely to be followed by a longer-lived ATP state in which the SH1 helix is unwound and the ATP is trapped (6).

The near-rigor conformation is the crystallographic structure that most closely resembles a strong actin-binding state. Thus, the position of the ELC in the nucleotide-free scallop structure seems to be similar to that found in electron-microscope images of actin decorated with nucleotide-free smooth myosin (16). In this view, the transition between the prepower stroke and the near-rigor conformations would correspond closely to the power stroke of the actomyosin cycle. In the case of scallop S1, the step size is about 120 Å, with a very small azimuthal component (see Fig. 2). (Note that this estimate is made by using the same isoform for the two states.) The flexible joint at the pliant region weakens the coupling between the torque generated by the MD and the motion of the lever arm.

In summary, our results indicate that the most stable conformations of scallop S1 seem to be the near-rigor state in the absence of nucleotide, and the transition state when ADP·Pi analogs are bound. In the absence of actin, ADP can induce both the near-rigor and the detached conformations, and when ATP analogs are bound, the detached state is the most favored conformation. Thus, scallop myosin is an exceptional system, allowing us to detect the influence of the content of the nucleotide-binding site on the conformation of the myosin head in the absence of actin. The current study also reveals that conformations probably common to many isoforms may be experimentally accessible (i.e., by crystallography) only in cer-

tain isoforms and under certain conditions. But it is also plain that certain isoforms may exist in specialized conformations not observed for other isoforms, because of structural features related to specific functions. A good example here is ADP release in vertebrate smooth muscle S1 (16) and some unconventional myosins (18) that could lead to the production of movement of the lever arm in two distinct steps (19). Similarly, the study of unconventional myosins, such as myosin VI, should reveal whether the conformational changes observed in the MD of myosin II characterize the whole superfamily and how the insertion of ≈50 residues in this motor allow it to move with reverse polarity (20). Thus, a thorough study of a variety of myosin isoforms is a productive approach to visualizing the multiple steps in the actomyosin cycle.

We thank Hugh Huxley for comments on the manuscript; Yale Goldman, Emil Reisler, and Daniel Himmel for discussions; Roberto Dominguez, Niels Volkmann, and the staff at the Cornell High Energy Synchrotron Source for help with data collection; Carol Palmer and Andrew Brilliant for assistance with photography; and Linda Lynch for devotion to the manuscript. This work was supported by grants from the National Institutes of Health and the Muscular Dystrophy Association (to C.C.), a grant from the National Institutes of Health (to A.G.S.-G.), as well as postdoctoral fellowships from the Human Frontier Sciences Program Organization and the Association Française Contre les Myopathies (to A.H.).

1. Rayment, I., Rypniewski, W. R., Schmidt-Bäse, K., Smith, R., Tomchick, D. R., Benning, M. M., Winkelmann, D. A., Wesenberg, G. & Holden, H. M. (1993) *Science* **261,** 50–58.
2. Fisher, A. J., Smith, C. A., Thoden, J. B., Smith, R., Sutoh, K., Holden, H. M. & Rayment, I. (1995) *Biochemistry* **34,** 8960–8972.
3. Smith, C. A. & Rayment, I. (1996) *Biochemistry* **35,** 5404–5417.
4. Gulick, A. M., Bauer, C. B., Thoden, J. B. & Rayment, I. (1997) *Biochemistry* **36,** 11619–11628.
5. Dominguez, R., Freyzon, Y., Trybus, K. M. & Cohen, C. (1998) *Cell* **94,** 559–571.
6. Houdusse, A., Kalabokis, V. N., Himmel, D., Szent-Györgyi, A. G. & Cohen, C. (1999) *Cell* **97,** 459–470.
7. Gulick, A. M. & Rayment, I. (1997) *BioEssays* **19,** 561–569.
8. Holmes, K. C. (1998) *Novartis Found. Symp.* **213,** 76–92.
9. Otwinowski, Z. & Minor, W. (1993) in *Data Collection and Processing*, eds. Sawyer, L., Isaacs, N. & Bailey, S. (CRC Daresbury Laboratory, Warrington, U.K.), pp. 59–62.
10. Navaza, J. (1994) *Acta Crystallogr. A* **50,** 157–163.
11. Jones, T. A., Zou, J.-Y., Cowan, S. W. & Kjeldgaard, M. (1991) *Acta Crystallogr. A* **47,** 897–904.
12. Houdusse, A. & Cohen, C. (1996) *Structure (London)* **4,** 21–32.
13. Rayment, I., Holden, H. M., Whittaker, M., Yohn, C. B., Lorenz, M., Holmes, K. C., Milligan, R. A. (1993) *Science* **261,** 58–65.
14. Taylor, E. W. (1991) *J. Biol. Chem.* **266,** 294–302.
15. Walker, M., Zhang, X. Z., Jiang, W., Trinick, J., White, H. D. (1999) *Proc. Natl. Acad. Sci. USA* **96,** 465–470.
16. Whittaker, M., Wilson-Kubalek, E. M., Smith, J. E., Faust, L., Milligan, R. A. & Sweeney, H. L. (1995) *Nature (London)* **378,** 748–751.
17. Dobbie, I., Linari, M., Piazzesi, G., Reconditi, M., Koubassova, N., Ferenczi, M., Lombardi, V. & Irving, M. (1998) *Nature (London)* **396,** 383–387.
18. Jontes, J. D., Wilson-Kubalek, E. M. & Milligan, R. A. (1995) *Nature (London)* **378,** 751–753.
19. Veigel, C., Coluccio, L. M., Jontes, J. D., Sparrow, J. C., Milligan, R. A. & Molloy, J. E. (1999) *Nature (London)* **398,** 530–533.
20. Wells, A. L., Lin, A. W., Chen, L. Q., Safer, D., Cain, S. M., Hasson, T., Carragher, B. O., Milligan, R. A. & Sweeney, H. L. (1999) *Nature (London)* **401,** 505–508.
21. Geeves, M. A. (1991) *Biochem J.* **294,** 1–14.